

EFFECT OF INTERMOLECULAR FORCES ON THIN FILM INSTABILITY

Emily M. Tian

Department of Mathematics and Statistics

Wright State University

Dayton, OH, 45435, USA

Abstract: We consider the effect of van der Waals intermolecular forces on instability problems occurring in thin liquid film pattern formation induced by an electric field. The physical setup is a layer of thin liquid film sandwiched between two electrodes and separated by an air gap from the top mask electrode. We formulate the nonlinear parabolic fourth order thin film equation by deriving van der Waals forces, electric induced forces and incorporate the surface tension in the model. In the long wavelength limit, we find that perturbations at the interface undergo regulated dynamics and the initial film thickness plays a critical role in the pattern formation process.

AMS Subject Classification: 35B36, 65P40, 76A20, 76E17

Key Words: thin film, stability, intermolecular forces, electric field

1. Introduction and Model Formulation

In a lithographically induced self-assembly (LISA [2]) process, the application of an electrostatic force is used to create and replicate lateral structures in polymer films on a submicrometer length scale, [14]. The instability is triggered by intermolecular van der Waals attractions or by an electric field or simply a temperature gradient. The thin film patterning finds important appli-

cations in fabrication of optical or electronic devices, sensors or biochips, [20]. The physical configuration consists of a layer of a smooth thin polymer film cast on a flat silicon substrate. A pattern-free mask is placed above the film at a distance less than $1\mu m$, leaving a thin air gap. The bottom substrate is completely wettable. The system is heated above the glass transition temperature of the polymer liquid and allowed to cool down to room temperature. An external electric field is supplied vertically onto the substrate and mask to produce a uniform interfacial electrostatic pressure that drives the film layer to flow away from the less wettable region, thus destabilize the film surface. Incorporating with the surface tension on the interface of the film that tends to stabilize the flow, the electric field can induce sufficiently long wavelength fluctuations and produce a well controlled patterns to appear on the film surface. Such electric field induced instability is characterized by a hexagonally ordered pattern, [14]. When the two electrodes are at a fixed distance, and the initial film thickness is adjusted from thinner ($93nm$) to thicker ($193nm$), the lateral hexagonal packing becomes more orderly, clear, and complete, [14]. At the mean time, it was observed that without externally applied electric gradient, the intermolecular interactions alone would either keep the film stable, or for significantly long time, the film could break up to form random irregular interface shapes [14, 17]. Nazaripoor [8] reported a combined thermocapillary-electrohydrodynamic approach to create nano sized features, that incorporates a bounding fluid and heat distribution from the bottom substrate to increase the number density of pillars thus reduce the characteristic length scale λ_{max} of these pillars. Their study revealed a good balance between thermal, EHD and surface tension controls the growth of the film patterns.

Gravitational effects are negligible due to the very small thickness of the film. The intermolecular forces, including van der Waals attraction and extremely short range Born repulsion are considered here, [20]. The electric field induced pattern generation process has stimulated much work toward understanding the underlying mechanism because of its ability to create patterns at micro and nano scales, both spontaneously and under a guide from a grated mask.

If the top mask is engraved with a pattern form, then the electric field will vary laterally, so that a well guided replication from the mask can appear on the film surface. The electric field can control and organize the replication of a master pattern from the mask onto the thin film surface; the theoretical explanation to this phenomenon is limited to a linear analysis to examine the initial stage instability; most activity in this area is incorporated with numerical simulations, [5, 7, 21]. It was found that thick films ($23\mu m$) supplied with large

electric voltage (150V) are essential for a faithful replication of the master pattern, [5].

Consider a thin liquid layer of mean thickness h_0 spin-coated onto a planar silicon substrate located at $z = 0$ and bounded above by an interface satisfying $z = h(x, y, t)$, where (x, y, z) represents a laboratory coordinate system and t is time. A planar silicon mask is mounted at a distance d from the bottom, leaving a thin air gap to separate from the film surface. The system is applied a constant electrostatic potential U . We assume the polymer is of relatively low molecular weight so that gravity may be neglected while the flow is slow enough so that a continuum mechanical approach is valid. The dimensionless dielectric constants of the polymer film and air are taken to be ϵ_p and $\epsilon_a = 1$, respectively. The long term behavior of the liquid is insensitive to the initial conditions.

In the long wavelength limit [9, 17], the following spatiotemporal equation describes the thin film evolution of the film interface $z = h(x, y, t)$:

$$3\mu \frac{\partial h}{\partial t} - \nabla \cdot [h^3 \nabla p] = 0, \quad (1)$$

where μ is the constant viscosity of the polymer and p is the pressure distribution across the interface, which consists of the atmospheric pressure p_0 , the surface tension, the intermolecular interaction p_i and the electrostatic pressure p_e . In short,

$$p = p_0 - \gamma \nabla^2 h + p_i + p_e. \quad (2)$$

2. Van der Waals Forces

Although the instability is caused mostly from the competition between the surface tension and the electrostatic effects, the van der Waals intermolecular forces become more prominent as the technical demand for thinner film deposition and smaller film features has increased; therefore, our interest in this paper is to fully account for the role played by the intermolecular interactions in the complete evolution process.

Molecules attract one another when they are far apart and repel one another when close; the intermolecular forces therefore exist in two different forms: the long range attractions operate when molecules are sufficiently far apart at distance where their electron clouds overlap insignificantly so the effects of electron exchange are negligible, they decrease at a power of $1/r$; while the short range repulsion forces result from the cloud overlap, they originate in the coulomb and exchange interactions and increase exponentially with decreasing

r , are significant when two bodies come close. The interaction potential energy $u(r)$ is represented as a function of separation distance r , and the effective force is $p_i = -\frac{du(r)}{dr}$ (see Buckingham [1]). Between macroscopic bodies, the van der Waals force takes the form of $p_i(r) = -\frac{C}{r^n}$, which represents an attraction when it is a negative force with $C > 0$; while for $C < 0$, it becomes a positive force that stands for a repulsion [4].

Van der Waals long-range attractions can be important at the initial stage on the solid-liquid and liquid-gas interfaces. We assume that the substrate is wettable so that the attraction between substrate and film stabilizes the film layer initially until the electric field is applied that triggers an instability to take place. We represent this attraction as $F_{vdw} = -\frac{A}{h^3}$, with the effective Hamaker coefficient A ranging from 10^{-21} to $10^{-22}J$ depending on polymer properties [4, 22].

At the later stage development when the film surface rises close to the top mask, a short range Born repulsion between the film surface and the mask becomes effective that ensures non-penetration of the film at the contact with the top mask. We use $F_{br} = \frac{B}{(d-h)^3}$ with $B > 0$ to represent this repulsion in p_i , where B is typically determined by setting $p_i = 0$ at a cut off thickness where $d-h \approx 1nm$. Considering the fact that the accurate values of the Hamaker constants do not affect the dynamics qualitatively, we will take $A = B$ to simplify the analysis [21]. In a summary, our $p_i = -\frac{A}{h^3} + \frac{A}{(d-h)^3}$, with $A > 0$.

The surface tension tends to minimize the area of the film-air interface, thus stabilizing the polymer film. In opposition to this, the electric field destabilizes the film by acting on the polarization field and free charge at the interface.

3. Electrostatic Pressure

The component of the electrostatic pressure in the equation (1) has been carefully derived in Tian [18]; for the completeness of this paper, we revisit most part of the derivation process. Following the formulation of Saville [13], under static conditions, electric and magnetic phenomena are independent since their fields are uncoupled. Maxwell's equations can be simplified by neglecting magnetic fields due to the fact that the magnetic phenomena time scale is much shorter than that of electrical phenomena. The net charge in the liquid layer and in the air layer may be assumed to be zero: $\nabla \cdot \vec{E}_j = 0$, ($j = p, a$), where \vec{E}_j

represent the electric field strength in each layer. There exists the potential Ψ_j such that $\vec{E}_j = -\nabla\Psi_j$ under the condition $\nabla \times \vec{E}_j = 0$, so a Laplace equation for the potential reads as: $\Psi_j: \nabla^2\Psi_j = 0$; in the long wave limit, it simplifies to the following:

$$\frac{\partial^2\Psi_p}{\partial z^2} = 0, \quad \frac{\partial^2\Psi_a}{\partial z^2} = 0. \quad (3)$$

The boundary conditions at the two solid plates are:

$$\Psi_p = U \quad \text{at } z = 0, \quad \text{and} \quad \Psi_a = 0 \quad \text{at } z = d. \quad (4)$$

The balance of Ψ_j and the zero surface charge on the interface require that

$$\Psi_a = \Psi_p, \quad \text{and} \quad \|\epsilon E\| = \epsilon_p E_p - \epsilon_a E_a = 0 \quad \text{at } z = h(x, y, t), \quad (5)$$

where $\|\cdot\|$ denotes the jump of the dielectric displacement ϵE across the interface.

Solving equation (3) with the boundary conditions (4) and (5) yields:

$$E_p = \frac{U}{\epsilon_p d - (\epsilon_p - 1)h} \quad \text{and} \quad E_a = \frac{U\epsilon_p}{\epsilon_p d - (\epsilon_p - 1)h}. \quad (6)$$

The electrostatic and hydrodynamical phenomena are coupled through the Maxwell stress tensor. The applied electric field produces a pressure p_e on the surface of the thin film, which is equal to the jump of the isotropic components of the Maxwell electrical stress tensor [3, 13]:

$$p_e = \frac{1}{2} \|\epsilon E^2\| = \frac{\epsilon_0}{2} (\epsilon_p E_p^2 - \epsilon_a E_a^2) = -\frac{\epsilon_0 \epsilon_p (\epsilon_p - 1) U^2}{2[\epsilon_p d - (\epsilon_p - 1)h]^2}, \quad (7)$$

where ϵ_0 is the vacuum dielectric permittivity.

4. Nondimensionalization and Stability Analysis

Introducing the scale factor $\frac{\mu d^2}{\epsilon_0 U^2}$ for time: $\bar{t} = t/(\frac{\mu d^2}{\epsilon_0 U^2})$, and d for both length and film thickness: $\bar{h} = h/d$, we non-dimensionalize the governing interface equation as follows where we use the same symbols to represent the corresponding dimensionless quantities:

$$\begin{aligned} h_t + \alpha \nabla \cdot [h^3 \nabla (\nabla^2 h)] + \beta \nabla \cdot [h^3 (\epsilon_p - (\epsilon_p - 1)h)^{-3} \nabla h] \\ - \eta \nabla \cdot [h^3 (h^{-4} + (1 - h)^{-4}) \nabla h] = 0, \end{aligned} \quad (8)$$

where

$$\alpha = \frac{\gamma d}{3\epsilon_0 U^2}, \quad \beta = \frac{\epsilon_p (\epsilon_p - 1)^2}{3}, \quad \eta = \frac{A}{\epsilon_0 d U^2}$$

are three dimensionless parameters.

A linear stability analysis can be employed to study the evolution of the interface between a polymer film and an air gap [14, 15], or between two layers of polymer film [6]. The critical wave length λ is typically examined to predict the onset of the destabilizing process [11, 12]. In the cases involving leaky dielectric films, conductivity and the thickness ratio are found to be critical parameters [10, 16]; in the case of perfect films, the thickness ratio of the air gap to the film is an important control parameter [14, 20]. In order to explain this pattern formation process more fully, a thorough investigation is needed to analyze nonlinear factors. Tian [19] has conducted a weakly nonlinear analysis and numerical simulations on the model without intermolecular forces and discovered the dependence of the pattern formation on the thickness ratio, for a nonconducting thin film.

In order to find the critical wavenumber when instabilities occur, we perform a linear stability analysis on the one dimensional model:

$$\begin{aligned} h_t + \alpha[h^3 h_{xxx}]_x + \beta[h^3(\epsilon_p - (\epsilon_p - 1)h)^{-3} h_x]_x \\ - \eta[h^3(h^{-4} + (1 - h)^{-4})h_x]_x = 0. \end{aligned} \quad (9)$$

Consider a small perturbation H to the initial film thickness h_0 :

$$h = h_0 + H, \quad |H| \ll h_0, \quad (10)$$

and

$$H \propto e^{\sigma t} e^{ikx}, \quad (11)$$

where k is the wavenumber; σ is the growth rate and h_0 the nondimensional version of the initial uniform film thickness.

Substituting the solution of (10), (11) into equation (9), we obtain the dispersion relation between σ and k to the first order of perturbation:

$$\sigma(k^2) = h_0^3 k^2 [\beta(\epsilon_p - (\epsilon_p - 1)h_0)^{-3} - \eta(h_0^{-4} + (1 - h_0)^{-4}) - \alpha k^2], \quad (12)$$

from which the critical wavenumber when the onset of instability takes place is deduced to be:

$$k_0^2 = \frac{\beta}{\alpha}(\epsilon_p - (\epsilon_p - 1)h_0)^{-3} - \frac{\eta}{\alpha}(h_0^{-4} + (1 - h_0)^{-4}) \quad (13)$$

by considering $\sigma(k^2) = 0$. There follows the dispersion relation:

$$\sigma(k^2) = \alpha h_0^3 k^2 [k_0^2 - k^2], \quad (14)$$

that behaves in the quadratic form of k^2 .

Equation (13) suggests that the instability depends only on the initial film thickness once the dielectric material is chosen therefore ϵ_p is determined, the electrodes are kept at a fixed distance d , and the electric potential U is prescribed.

To make a good comparison with the past work by Tian [19], we are taking the same set of representative value [15, 20]:

$$\begin{aligned}\epsilon_0 &= 8.854 \times 10^{-12} C^2 / Nm^2, U = 70V, \\ \epsilon_p &= 2.5, \gamma = 3.8mN/m, d = 100nm,\end{aligned}\tag{15}$$

together with the Hamaker constant $A = 10^{-21} J$.

The dependence of k_0^2 on h_0 with and without the consideration of intermolecular forces is compared on three different intervals of the initial film thickness, and is depicted in Fig 1. For $h_0 \in (0.16, 0.96)$, the van der Waals forces seem to have no influence on determining the critical wavenumber; while for the film thinner than 0.16 or thicker than 0.96, the significance of the intermolecular effect is obviously prominent. Note that h_0 is a rescaled quantity of film thickness to the electrodes depth d , this finding of h_0 interval provides us with a useful information of adjusting and controlling the experimental parameters.

5. Conclusion and Discussions

The case of a patternless mask has been considered in this paper. The result has explained the intermolecular effects contributing to instability of thin liquid film at the initial exponential development stage. Controlled by an electrostatic field, it is discovered that the relative thin film thickness is crucial in driving the patterning process.

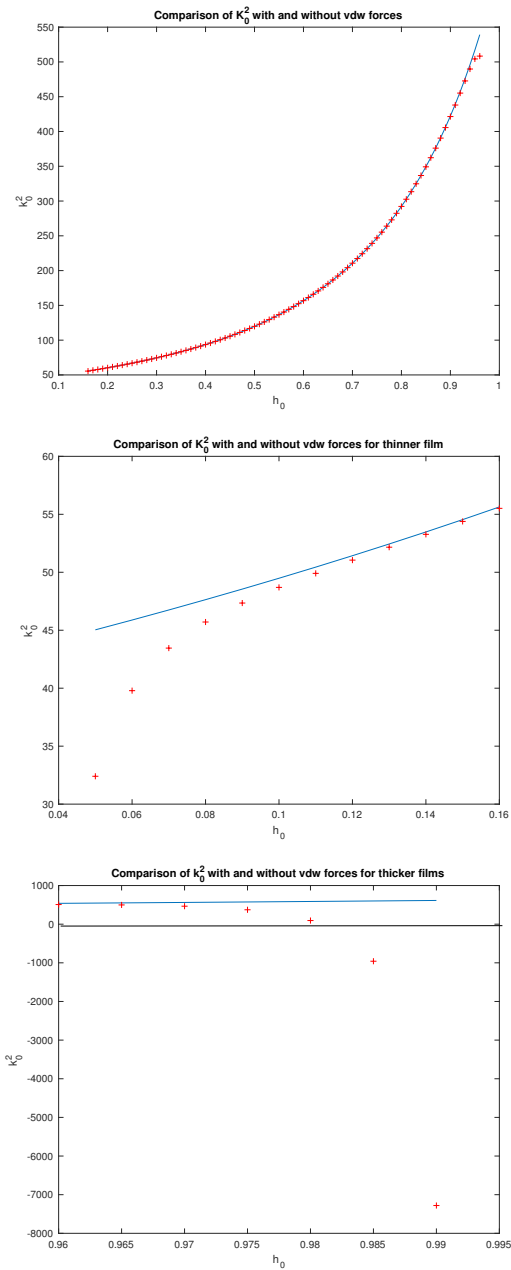


Figure 1: The curves with + are for k_c^2 with vdw effects.

References

- [1] A.D. Buckingham, Intermolecular forces, *Phil. Trans. R. Soc. Lond. B*, **272** (1975), 5-12.
- [2] S.Y. Chou, L. Zhuang, Lithographically induced self-assembly of periodic polymer micropillar arrays, *J. Vac. Sci. Technol. B*, **17**, No 6 (1999), 3197-3202.
- [3] L.D. Landau, E.M. Lifshitz, *Electrodynamics of Continuous Media*, Pergamon Press (1960).
- [4] F.L. Leite, C.C. Bueno et al., Theoretical models for surface forces and adhesion and their measurement using atomic force microscopy, *Int. J. Mol. Sci.*, **13** (2012), 12773-12856.
- [5] H. Li, W. Yu et al., Faithful replication of grating patterns in polymer through electrohydrodynamic instabilities, *J. Micromech. Microeng.*, **24** (2014).
- [6] Z. Lin et al., Electric field induced instabilities at liquid/liquid interfaces, *Journal of Chemical Physics*, **114**, No 5 (2001), 2377-2381.
- [7] H. Nazaripoor, C.R. Koch et al., Compact micro/nano electrohydrodynamic patterning: using a thin conductive film and a patterned template, *Soft Matter*, **12** (2016), 1074-1084.
- [8] H. Nazaripoor, C.R. Koch et al., Thermo-electrohydrodynamic patterning in nanofilms, *Langmuir* (2016), 5776-5796.
- [9] A. Oron, S.H. Davis, S.G. Bankoff, Long-scale evolution of thin liquid films, *Reviews of Modern Physics*, **69**, No 3 (1997), 931-980.
- [10] L.F.III Pease, W.B. Russel, Linear stability analysis of thin leaky dielectric films subjected to electric fields, *Journal of Non-Newtonian Fluid Mechanics*, **102** (2002), 233-250.
- [11] L.F. III Pease, W.B. Russel, Electrostatically induced submicron patterning of thin perfect and leaky dielectric films: a generalized linear stability analysis, *Journal of Chemical Physics*, **118**, No 8 (2003), 3790-3803.
- [12] L.F.III Pease, W.B. Russel, Limitations on length scales for electrostatically induced submicrometer pillars and holes, *Langmuir*, **20** (2004), 795-804.

- [13] D.A. Saville, Electrohydrodynamics: the Taylor-Melcher leaky dielectric model *Annu. Rev. Fluid Mech.*, **29** (1997), 27-64.
- [14] E. Schäffer, T. Thurn-Albrecht, T.P. Russell and U. Stelner, Electrically induced structure formation and pattern transfer, *Nature*, **403** (2000), 874-877.
- [15] E. Schäffer, T. Thurn-Albrecht, T.P. Russell and U. Stelner, Electrohydrodynamic instabilities in polymer films, *Europhysics Letters*, **53**, No 4 (2001), 518-524.
- [16] V. Shanker, A. Sharma, Instability of the interface between thin fluid films subjected to electric fields, *Journal of Colloid and Interface Science*, **274** (2004), 294-308.
- [17] E.M. Tian, D.J. Wollkind, Nonlinear stability analyses of pattern formation in thin liquid films, *Interfaces and Free Boundaries*, **5** (2003), 1-25.
- [18] E.M. Tian, Pattern formation induced by an electric field in thin liquid films, *Journal of Mathematics, Statistics, and Allied Fields*, **1**, No 1 (2007).
- [19] E.M. Tian, T.P. Svobodny and J.D. Phillips, Stability of thin film patterns induced by electro-static field, *International Journal of Applied Mathematics*, **24**, No 2 (2011), 221-228.
- [20] R. Verma, A. Sharma, K. Kargupta and J. Bhaumik, Electric field induced instability and pattern formation in thin liquid films, *Langmuir*, **21**, No 8 (2005), 3710-3721.
- [21] N. Wu, L.F. Pease and W.B. Russel, Electric-field-induced patterns in thick polymer films: weakly nonlinear and fully nonlinear evolution, *Langmuir*, **21** (2005), 12990-12302.
- [22] N. Wu and W.B. Russel, Dynamics of the formation of polymeric microstructures induced by electrohydrodynamic instability, *Applied Physics Letters*, **86** (2005), 241912.